International Journal of Sustainable and Green Energy
2024, Vol. 13, No. 3, pp. 43-57
https://doi.org/10.11648/j.ijrse.20241303.11

Research Article

Thermophysical and Mechanical Characterization of the Earth-Straw Materials Employed in the Building of Shell Houses in the Mourla Region of Cameroon's Far North

Bernard Kola[1, 2], Colbert Babé[2, *], Noël Djongyang[2]

[1]Energy Research Laboratory, Institute for Geological and Mining Research, Yaoundé, Cameroon

[2]Department of Renewable Energy, National Advanced School of Engineering of Maroua, University of Maroua, Maroua, Cameroon

Abstract

Using modern materials such as cement in construction leads to high energy consumption due to increased heat transfer, resulting in warmer indoor environments. In the hot climate of the Sudano-Sahelian zone in northern Cameroon, it is crucial to use materials that provide thermal comfort and reduce the need for air conditioning. Certain locally sourced materials support environmental preservation and facilitate the construction of houses for artisans. This research focuses on developing and characterizing bio-based products using raw earth. The study investigated the mechanical performance in compression, thermal conductivity, and other material properties. Different proportions of plant aggregates, ranging from 0% to 15% of the soil mass, were incorporated for the experimental study. The results indicate that the compressive strength values are 6.3, 8.5, 6.1, and 5.6 MPa for 0%, 5%, 10%, and 15% reinforcement, respectively, revealing a 35% increase in compressive strength with the addition of 5%. Furthermore, the study showed a 45% decrease in thermal conductivity compared to samples without reinforcement. These findings demonstrate that this eco-friendly material has the potential to promote the efficient use of local resources in the construction sector. It not only enhances thermal comfort and reduces energy consumption associated with air conditioning but also supports the construction of more sustainable buildings, leading to a cleaner environment.

Keywords

Thermophysical Properties, Thermal Conductivity, Compressive Strength, Earth Material, Traditional Housing

1. Introduction

The most effective way to achieve sustainable energy system development is to reduce the use of all energy resources. The untapped potential for energy conservation can have positive economic and environmental impacts. Conserving energy is essential for mitigating climate change. Whether residential or industrial, most buildings require significant energy to maintain a comfortable temperature. In warm climates like Cameroon, air conditioning is necessary for thermal comfort. However, utilizing natural cooling techniques can reduce the need for air conditioning, which is financially important in warm nations. Foreign architectural norms unsuitable for warm weather conditions are often used in con-

*Corresponding author: babecolbert@gmail.com (Colbert Babé)

Received: 9 August 2024; **Accepted:** 5 September 2024; **Published:** 26 September 2024

struction. The building sector accounts for 40% of global energy consumption and is increasing annually, according to the United Nations (2010) and the World Energy Outlook (2009). This significantly affects the environment and contributes to changes in global climate patterns. [1].

It has been recognized that utilizing materials with minimal environmental impact could substantially decrease energy consumption during construction. According to [2], employing appropriate materials and construction techniques can reduce a building's energy usage by 17% and its CO_2 emissions by 30%. Their transportation significantly influences the environmental impact of building materials. Earth, with its locally sourced natural raw materials and beneficial hygrothermal properties, requires low energy consumption during production, as outlined in [3]. Soil is readily available and can be reused with minimal processing. Earth construction materials are typically located just beneath the topsoil.

Adding fibers to the mixture could have a significant impact, as suggested by [4]. Natural fibers are commonly used in the production of Earth concretes. According to [5], substituting natural or vegetable fibers for synthetic fibers can reduce weight, lower costs, and decrease energy consumption. Additionally, research has shown that these biodegradable and non-toxic fibers offer favorable thermal and acoustic insulation properties [5, 6]. There is considerable research interest in using fibers from local materials for construction and energy conservation purposes. Historically, shell huts have been renowned for regulating moisture levels and improving thermal comfort within the building. Additionally, their unique architectural design gives them significant aesthetic appeal. Since the 1960s, these huts have become a major tourist attraction known for their long-lasting nature. Local inhabitants easily construct these homes using readily available soil and straw. However, in recent times, Sub-Saharan Africa has transitioned from shell houses to using imported cement and concrete.

The northern region of Cameroon is situated in a hot zone within the Sahelian area, making it susceptible to desertification and experiencing high temperatures reaching up to 45 ℃ during intense heat periods. As a result, buildings constructed with cementitious materials, while durable, are ill-suited for this environment due to their poor thermal properties, which contribute to excess heat within the structure. Consequently, there is a growing trend towards constructing houses using locally available inexpensive materials that enhance the thermal comfort of the occupants. Shell huts have become increasingly prevalent in major cities of the Far North Region and tourist centers, catering to cultural and tourism interests. Despite their popularity, there is a lack of scientific data on the materials and construction techniques used in shell hut construction, hindering their large-scale development. The local population appreciates these shell huts, and they are sought after by tourists. Still, the absence of scientific knowledge about the materials used undermines their durability and internal thermal comfort.

This research represents the initial attempt to tackle this issue, utilizing soil specimens procured from the building in the municipality of Mourla and the locally prevalent and accessible plant aggregates thatching material. The objective of this work is to promote earthen constructions by using the local materials used to build shell huts. Indeed, it is a question of achieving control of the durability parameters and thermophysical properties of the materials often used empirically for constructing shell huts.

We have used soil mixed with vegetable fibres, all extracted from Mourla, where the craftsmen most commonly construct huts in shells. To bring the conditions of the sample formulations closer to what is widely practised by craftsmen, we have made 4 formulations with the combination of soil to which 0, 5, 10, and 15% plant fibre aggregates were added.

The samples obtained after de-moulding were dried for at least 21 days in the shade in the laboratory at an ambient temperature of 22 ℃ before proceeding with the mechanical, thermophysical and durability tests.

2. Materials and Methods

The substance utilized in construction, comprising a blend of soil and straw, originates from Mourla (Figure 1), located at geographical coordinates 10 ℃54'0" N and 15 ℃4'60" E in the Maga District of the Far North Region of Cameroon. The primary structures erected using this material are shell huts, as depicted in Figure 2. This soil was selected based on its prevalent usage by the indigenous community to construct traditional dwellings. The equipment for fabricating the test specimens comprises metallic mould, its accompanying components, and the hydraulic press. The mold is built from a steel plate that is 8 millimeters thick to endure the compressive force without experiencing any deformation. The presence of apertures at the die's upper and lower extremities facilitates filling the die and extracting the specimen after compaction. Utilizing a pair of metallic plates capable of sliding within the mould reduces the flattening of the surfaces of the specimen. The foundation consists of two boards with a thickness of 8 centimeters each. The hydraulic press utilized for compaction exhibits versatility to perform compression and flexure tests. Various combinations of soil and straw were used to create mixtures. The samples for the multiple tests were generated by preparing four distinct mixtures. The first sample type was solely soil and served as the control. The remaining three types of samples contained straw in varying proportions of 5%, 10%, and 15% by mass. The moisture level of the blends falls within the range of 15% to 20%. The specimens made available for analysis possess measurements of 10 centimeters in length, 10 centimeters in width, and 3 centimeters in height, respectively. The visual representation depicted in Figure 3 illustrates the physical characteristics of the specimens fabricated utilizing varying proportions of straw Figure 4. The specimens were subjected

to desiccation in an oven to remove any moisture that may have been present within the pores. Subsequently, their masses were quantified and conserved within plastic receptacles.

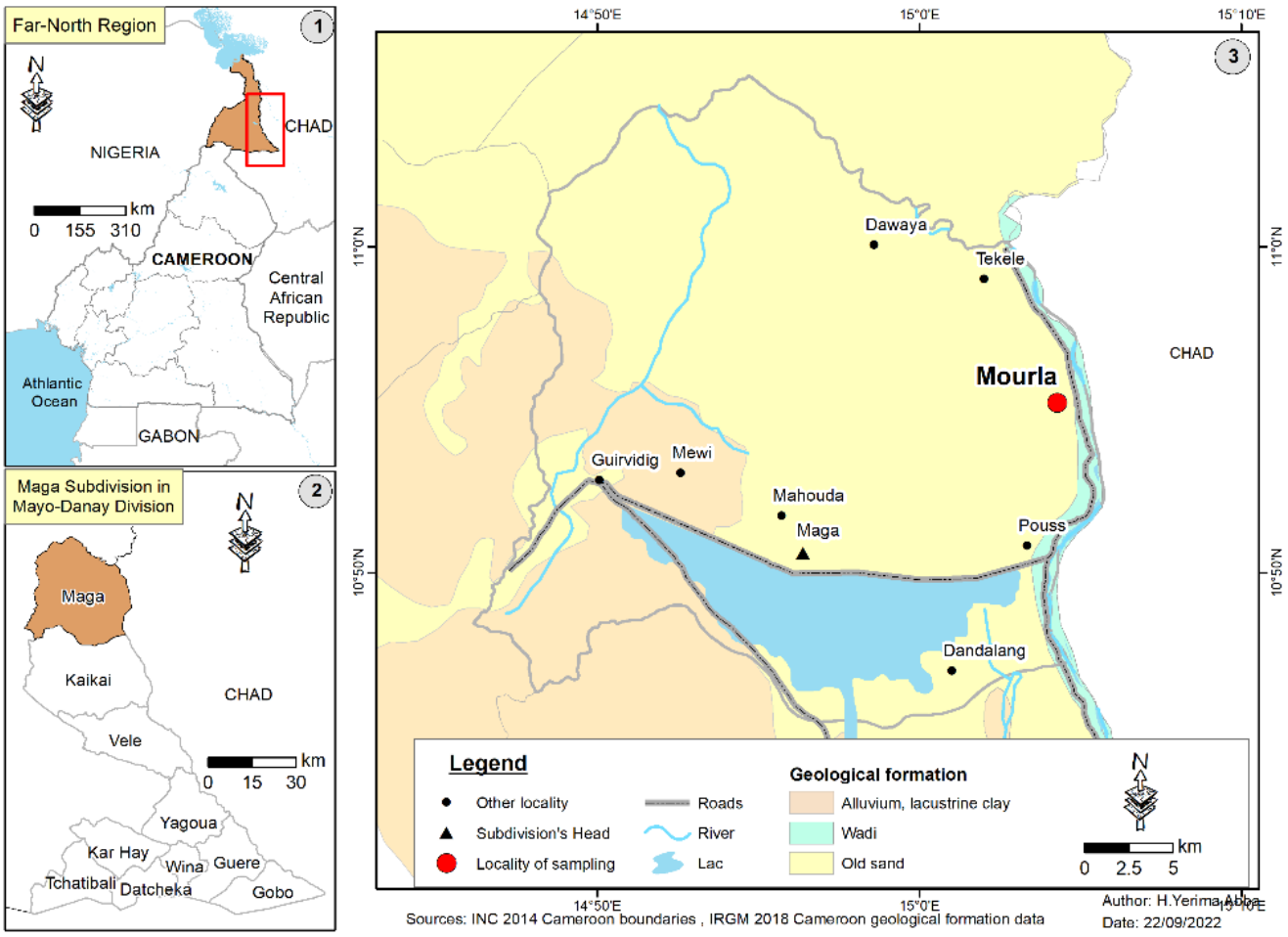

Figure 1. *Geographical location of study area.*

Figure 2. *Hut shell.*

Figure 3. Samples of research materials.

Figure 4. Plant aggregates.

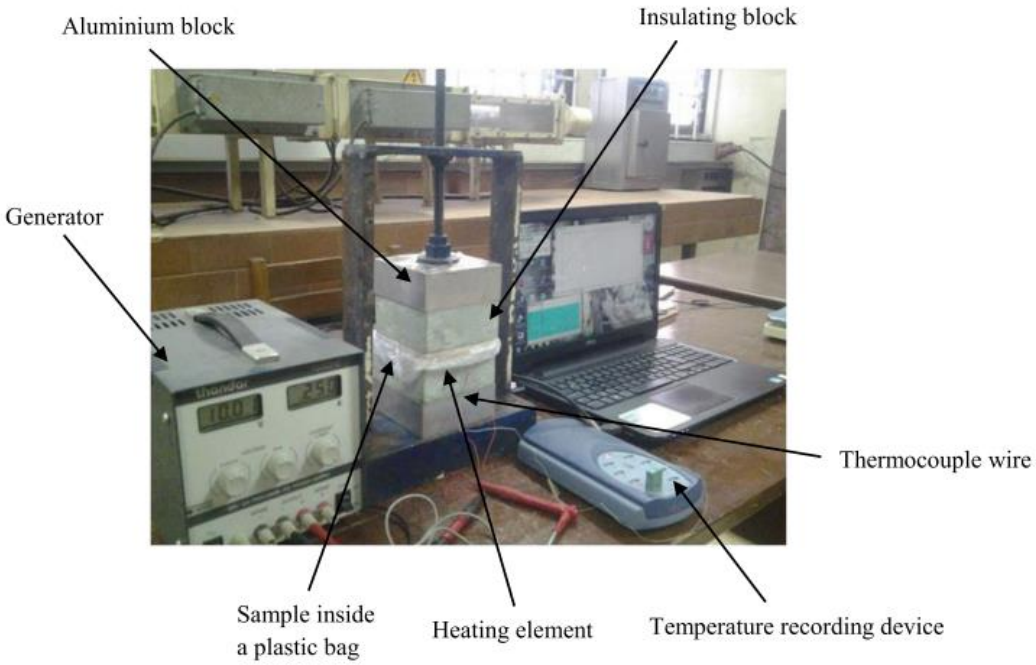

Figure 5. Experimental device.

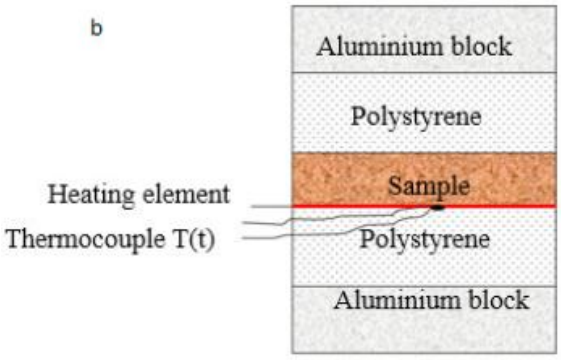

Figure 6. The experimental hot plate device.

2.1. Thermophysical Properties

2.1.1. Theoretical Approach to the Measurement of Thermophysical Properties

The asymmetric hot plane determines thermophysical properties, specifically thermal effusivity and volumetric heat capacity. The author effectively employed this approach [7]. The diagram depicted in Figure 5 illustrates the experimental configuration utilized for conducting the measurement. The thermal parameters are measured using processed samples with dimensions 10 cm x 10 cm x 3 cm. The specimens undergo a gradual drying process to decrease their moisture content. To prevent undesired alterations in weight, every sample is enclosed in plastic after each measurement.

2.1.2. Principle of the Asymmetric Hot Plane Method

The Asymmetric Hot Plane Method is a technique employed to ascertain the thermal conductivity of a given material between two isothermal planes (Figure 6). The experimental procedure involves situating the specimen to be analyzed onto a heating apparatus. Beneath the heating element, a polyethene insulating foam measuring 10 x 100 x 100 mm3 and possessing a conductivity of 0.04 $W.m^{-1}.K^{-1}$ is positioned to facilitate the transfer of most of the heat flow generated by the heating element through the sample. Subsequently, the assembly is inserted amidst a pair of aluminium blocks, each possessing high conductivity, with dimensions of 50 x 100 x 100 mm3. These blocks function as isothermal plates, thereby promptly facilitating the attainment of thermal equilibrium within the system. Thermocouples T_0, T_1, and T_2 are utilized to measure the temperature and positioned at the center of the faces of the sample and the insulating foam. Equation (1) provides the thermal conductivity λ_1 of the sample in a state of steady equilibrium.

$$\lambda_1 = \frac{e_1}{T_0 - T_1}\left[\frac{U^2}{R_\Omega . S} - \frac{\lambda_2}{e_2}\left(T_0 - T_2\right)\right] \tag{1}$$

The given parameters include e_1, representing the sample thickness; λ_2, denoting the thermal conductivity with a value of 0.04 $W.m^{-1}.K^{-1}$; and e_2, representing the thickness of the insulating foam with a value of 10 mm. Additionally, U refers to the voltage applied to the terminals of the heating element, which has an electrical resistance of RΩ=40 Ω and a surface area of S=0.0105 m^2. The experimental system was calibrated using a reference sample with a predetermined conductivity value.

The thermal effusivity of a sample is determined by utilizing the transient asymmetric hot plane method. The model of the system is predicated on the assumption of unidirectional (1D) heat transfer occurring at the core of the specimen. The temperatures of the aluminium blocks are presumed to be constant and equivalent, owing to the low heat flux that penetrates through the polystyrene and their substantial thermal capacities. By utilizing the quadrupole formalism, it is possible to express the model as follows:

$$\begin{bmatrix} \theta \\ \Phi_{01} \end{bmatrix} = \begin{pmatrix} 1 & 0 \\ c_h & 1 \end{pmatrix}\begin{pmatrix} 1 & R_c \\ 0 & 1 \end{pmatrix}\begin{pmatrix} A & B \\ C & D \end{pmatrix}\begin{pmatrix} A_i & B_i \\ C_i & D_i \end{pmatrix}\begin{bmatrix} 0 \\ \Phi_1 \end{bmatrix}$$

$$= \begin{pmatrix} A_1 & B_1 \\ C_1 & D_1 \end{pmatrix}\begin{bmatrix} 0 \\ \Phi_1 \end{bmatrix} \tag{2}$$

$$\begin{bmatrix} \theta \\ \Phi_{02} \end{bmatrix} = \begin{pmatrix} A_i & B_i \\ C_i & D_i \end{pmatrix}\begin{bmatrix} 0 \\ \Phi_2 \end{bmatrix} \tag{3}$$

$$\Phi_0 = \frac{\phi}{p} = \Phi_{01} + \Phi_{02} \tag{4}$$

θ is the Laplace transform of the temperature rise T(t);

Φ_{01} is the Laplace transform of the heat flux density dissipated by the heater to the sample (upwards);

Φ_{02} is the Laplace transform of the heat flux density dissipated by the heater to the polystyrene (downwards);

Φ_0 is the Laplace transform of the total heat flux density produced by the heater;

ϕ is the total heat flux density generated by the heater and C_h its heat capacity ($C_h = \rho_h . c_h . e_h$);

Rc is the contact resistance between the heater and the sample;

Φ_1 is the Laplace transform of the heat flux density reaching the aluminium block;

Φ_2 is the Laplace transform of the heat flux density reaching the lower aluminium block;

p is the Laplace parameter;

with:

$$A = D = \cosh\left(\frac{\rho c}{E} e\sqrt{p}\right);\quad B = \frac{\sinh\left(\frac{\rho c}{E} e\sqrt{p}\right)}{E\sqrt{p}};\quad C = E\sqrt{p}\sinh\left(\frac{\rho c}{E} e\sqrt{p}\right) \tag{5}$$

$$A_i = D_i = \cosh\left(\sqrt{\frac{p}{a_i}} e_i\right);\quad B_i = \frac{\sinh\left(\sqrt{\frac{p}{a_i}} e_i\right)}{\lambda_i\sqrt{\frac{p}{a_i}}};\quad C_i = \lambda_i\sqrt{\frac{p}{a_i}}\sinh\left(\sqrt{\frac{p}{a_i}} e_i\right) \tag{6}$$

The thermal effusivity of the sample is denoted by $E = \sqrt{\lambda \rho c}$, while the volumetric heat capacity of the sample is represented by ρc . Finally, the thickness of the sample is indicated by e. Additionally, the thermal conductivity, thermal diffusivity, and thickness of polystyrene are

represented by λ_i, a_i et e_i, respectively. By utilizing the relationship between the last five equations, the value of θ can be derived.

$$\theta(p) = \frac{\Phi_0(p)}{\frac{D_1}{B_1} + \frac{D_i}{B_i}} \tag{7}$$

The methodology employed in this approach involves estimating parameter values ($E, \rho c, R_c$ and C_h) by minimizing the squared error $\psi = \sum_{j=0}^{N} \left[T_{\exp}(t_j) - T_{\mathrm{mod}}(t_j) \right]^2$ between the theoretical values obtained via the inverse Laplace transformation of relation (7) and the corresponding experimental data points. The De Hoog algorithm [8] was utilized to perform the inverse Laplace transformation of relation (7).

2.2. Mechanical Properties

While these materials are primarily utilized for their thermal characteristics, they must possess a certain mechanical strength.

2.2.1. Compressive and Flexural Strength Tests

The compressive strength of a material refers to its ability to resist failure under a Newtonian load Figure 7. The formula for determining compressive strength is as follows:

$$R_c = \frac{F}{S} \tag{8}$$

Figure 7. *Compressive test.*

Mechanical Flexural Strength is the maximum stress it can withstand before experiencing failure under bending conditions. This technique is employed to ascertain the comparative variation in the bonding potency among constituent particles within a substance. The experiments follow the guidelines of ASTM F 417 - 1996, utilizing a three-point bending apparatus. The sample is dehydrated using an oven set at a temperature of 105 ℃ until a stable and unchanging weight is achieved. Following the cooling process, the object is positioned on a platen of a hydraulic press, supported by two parallel and horizontally oriented cylindrical structures. The platen is affixed to a piston that exhibits vertical movement. A dynamometer ring is connected to a crosshead, which supports a third cylindrical support that is symmetrical to the other two. This support is immobile and positioned above the specimen. The screen reading provides information regarding the magnitude of the load that resulted in the fracture. The equation for calculating bending strength in MPa is as follows:

$$\delta_f = \frac{3}{2}\frac{Pd}{le^2} \tag{9}$$

With

d: distance between cylindrical supports in mm, e: the thickness of the specimen in mm

P: load applied at a break in N, l: width of the specimen in m.

2.2.2. Abrasion Test

The present examination is employed to ascertain the level of abrasion resistance exhibited by clay bricks utilized in the construction of facing masonry Figure 8. The abovementioned parameter is not inherently linked to mechanical potency but typically strongly correlates with the soil's inherent characteristics. The specimen intended for examination is devoid of moisture. A wire brush with a weight of 6 kg is employed to cleanse the surface of the masonry facing that is exposed to precipitation. Each instance of the brush completing a full rotation is considered one cycle of scrubbing, and this process is repeated for a total of 50 cycles. The quantification process involves the determination of the weight of the substance eliminated by the brush. The material's dry weight is expressed per square centimetre of a brushed surface to obtain a test that is not dependent on the block's shape and size. Upon completion of the brushing process, the specimen is purged of any extraneous debris and subsequently quantified to ascertain the magnitude of the dislodged particulate matter.

$$m = mo - m1 \tag{10}$$

The brushing surface (S) is also calculated. $S = LI$ (11)

With:

L= Brushing surface (in cm);

I= width of the brush (in cm) equals the brushed width of the specimen.

The provided data can be used to determine each sample's abrasion coefficient. The abrasion coefficient, denoted as Ca, is the quotient of the brushed surface area (S) and the mass of material removed by brushing (g).

$$Ca\ (cm^2/g) = S/m \tag{12}$$

Figure 8. Abrasion test.

2.2.3. Water Absorption

The experiment involved conducting a test to ascertain the water absorption coefficient (A) of prismatic samples measuring 4 cm x 4 cm x 16 cm, which had been subjected to drying at a temperature of 60 ℃. The determination of the water absorption coefficient (A) was based on measuring the mass of water absorbed over time and the base area. The calculation of the water absorption coefficient (A) was carried out using the following formula:

$$A = \frac{m_1 - m_0}{S.\sqrt{t}} \quad (13)$$

With

m_0: mass of the dried sample, m_1: mass of the sample soaked in water for a time t

S: bottom base area (4x4) cm ^{2}of the sample, t: absorption time in seconds

Particle size analysis is typically the initial examination to determine the gauge's identification. [9].

3. Results and Discussion

3.1. Thermal Conductivity

The thermal conductivity values are 0.72, 0.54, 0.43, and 0.38 (W/(m. K)) for plant aggregates with 0, 5, 10, and 15% content, respectively. The addition of plant aggregates percentage from 0 to 15% causes a 45% decrease in thermal conductivity compared to sample without reinforcement. The relationship between fiber size and thermal conductivity is inverse, whereby an increase in fiber size decreases the material's thermal conductivity. Figure 9. This finding aligns with the inherent characteristic of cellulose as a material that provides thermal insulation. A strong correlation exists between the augmentation of total closed porosity in the material and the reduction in thermal conductivity. The thermal conductivity of a material is reduced due to the deceleration of heat conduction caused by air-filled voids within it. Figure 10 shows that the thermal conductivity logically increases with water content. The material being porous thermal conductivity coefficient of water being higher than that of air.

Minimizing thermal conductivity is advantageous for construction as it curtails the transmission of thermal energy from the exterior surroundings to the interior and regulates the indoor temperature. Implementing effective thermal comfort measures in buildings can reduce energy costs, particularly in Northern Cameroon, where such expenses can significantly burden most of the population. Authors widely acknowledge that including plant-based fibers or aggregates can effectively decrease the conductivity measurements of clay plasters [10-13]. The outcome mentioned above can be primarily elucidated by the augmentation in porosity and the reduction in density.

An inverse relationship exists between the quantity of plant material and thermal conductivity. The literature has extensively documented the enhancement of thermal insulation by incorporating plant aggregates [14-16]. This phenomenon can be attributed to the reduction in the density of the composite material. Composites' enhanced thermal insulation efficacy highlights the significance of investigating earth blocks incorporating plant aggregates. The findings of our study are consistent with the outcomes reported by Laborel [17].

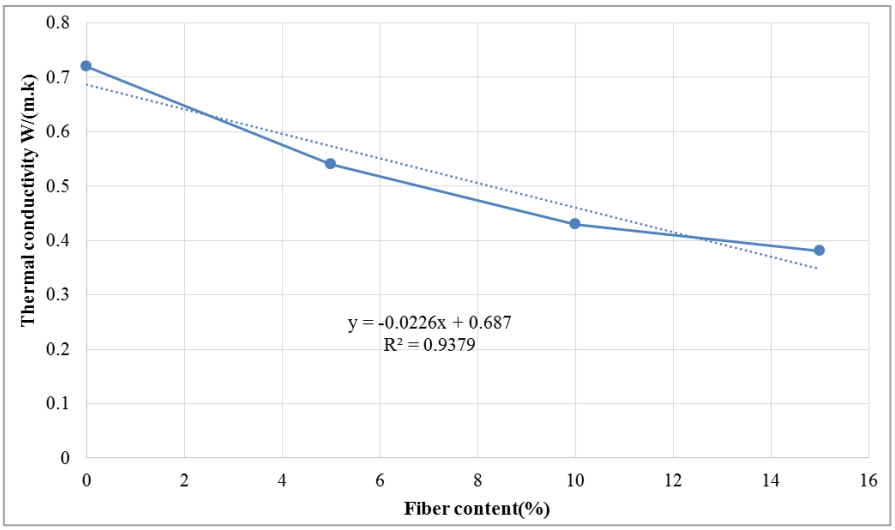

Figure 9. Thermal conductivity of the material as a function of fiber content.

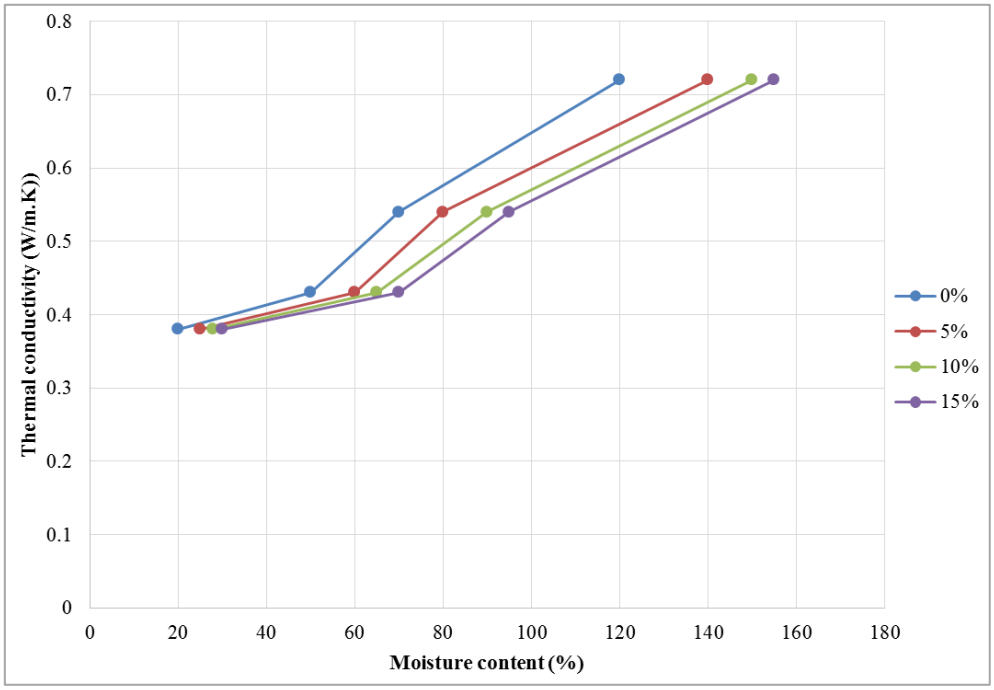

Figure 10. *Thermal conductivity of the material as a function of water content.*

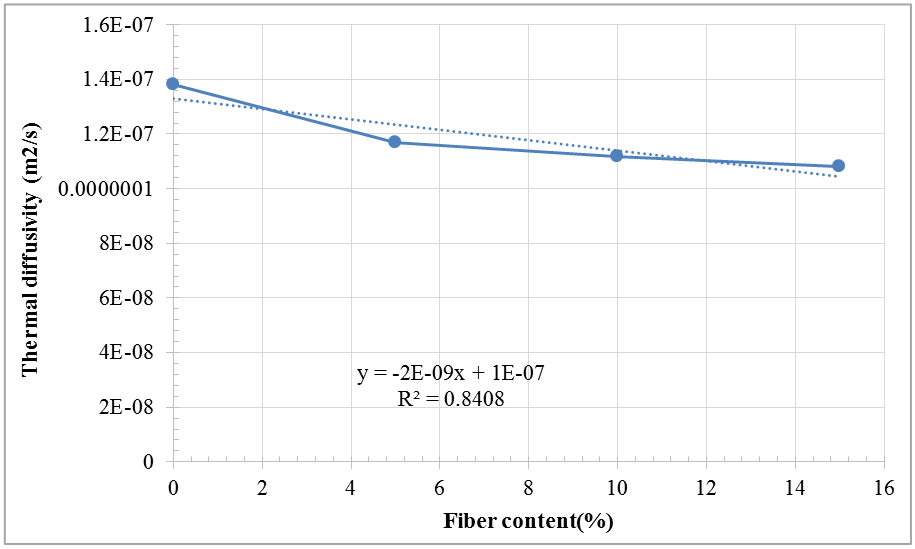

Figure 11. *Thermal diffusivity of the material as a function of fiber content.*

Figure 11 is a physical property that describes the rate at which heat diffuses through a material in response to a temperature gradient [18]. The abovementioned citation refers to the thermo-physical characteristic, which specifies the velocity at which thermal energy is transmitted via conduction in response to alterations in temperature. The trend observed in the evolution of thermal diffusivity is consistent with that of thermal conductivity, whereby the incorporation of fibers results in a decrease in thermal diffusivity. In contrast, an increase in the percentage of fiber addition leads to an increase in thermal diffusivity. The impact of the fibers' hollow structure and morphologies on heat transfer within the composite is a crucial factor that reduces the composite's thermal diffusivity and thermal conductivity. Thermal effusivity Figure 12 is a highly intriguing concept concerning the efficacy of thermal insulation materials. The aforementioned parameter pertains to the material's surface heat absorption and release capacity [19]. Therefore, the determination of thermal conductivity and diffusivity precedes calculating thermal effusivity values. It is worth noting that the thermal effusivity exhibits a decreasing trend as the fiber content increases. The present behaviour resembles the research.

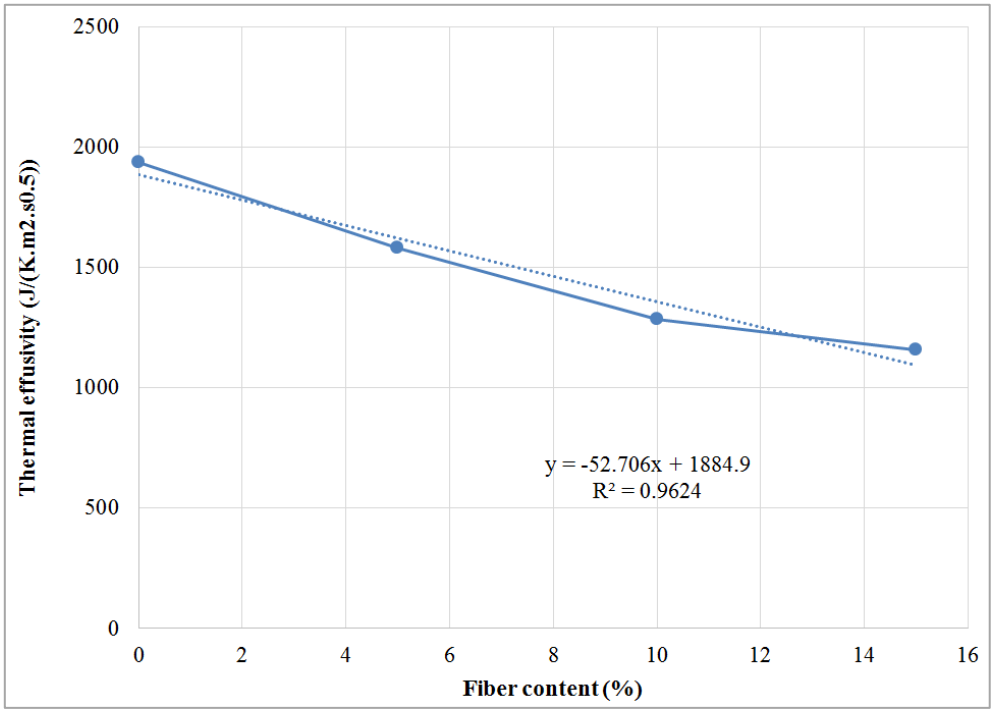

Figure 12. *Thermal effusivity of the material as a function of fiber content.*

The present behaviour resembles the research conducted by scholars cited as [6, 19-21], who investigated the impact of incorporating palm fibers into composites and concurred that such materials possess a reduced heat exchange capacity with their surroundings. The incorporation of 5% fiber results in a reduction of density in diverse composites. The decrease observed can be attributed primarily to the low weight of the integrated fibers and their porous composition, as noted in [19]. Furthermore, the augmentation of fiber content leads to a rise in the incorporation of air and voids within the composite material, as reported in [22]. As a result, these composite materials exhibit a notable weight reduction, as stated in [23].

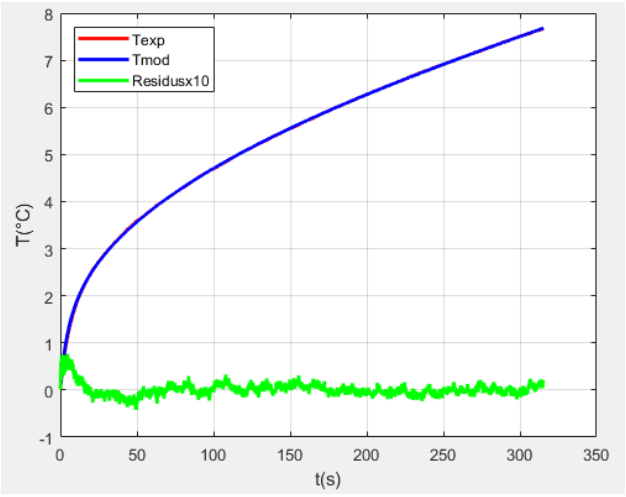

a. Experimental and modeled curves with residues

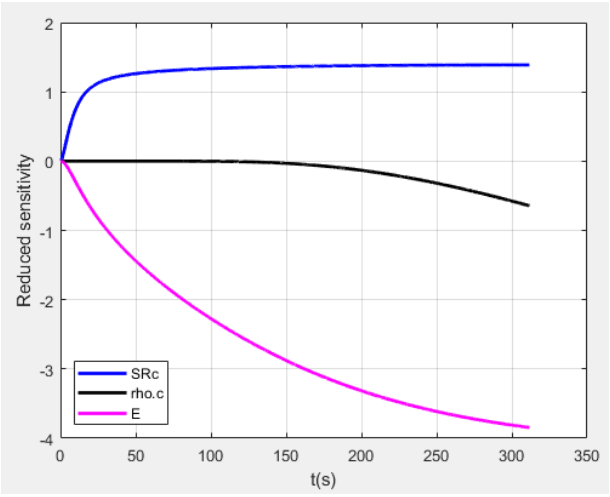

b. Reduced sensitivity

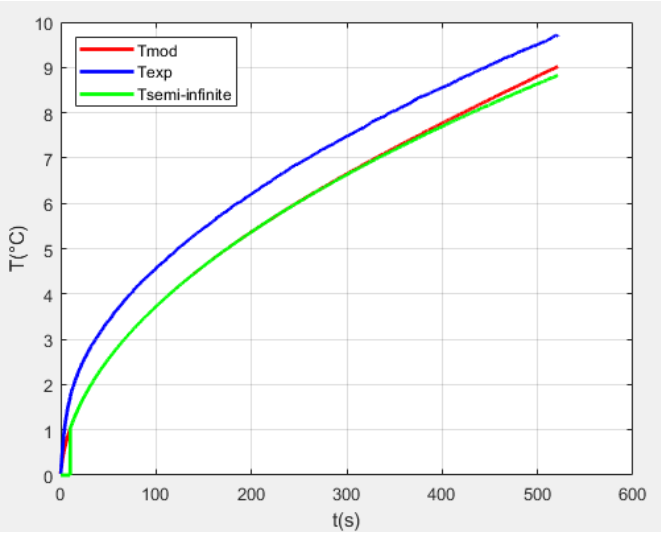

c. Evolution of temperatures

Figure 13. *Simulation curves for front and rear face temperatures and reduced sensitivities to each temperature as a function of time.*

Figure 13 (a) displays the outcome of the minimization process for the experimental and theoretical thermograms, along with their respective residuals, for the given sample. The empirical data aligns closely with the theoretical curve up to t=300s, indicating the soundness of the 1D model within the sample's central region [7]. The residual curve depicted in the figure indicates a high degree of proximity and complete overlap between the experimental curve in red and the model curve in blue, specifically within the temporal range of 0 to 320 seconds. At this juncture, the residuals exhibit a near-centralized distribution around the zero mark, and the transfer has persisted as unidirectional (1D). The impact of the initial thermal capacity of the heater on the heating process is discernible within the time frame of 0 to 5 seconds. Examining these curves indicates that the sample upholds the semi-infinite medium assumption, which posits that the perturbation has not yet propagated to the other side during the brief interval of 2 to 22 seconds.

The sensitivity analysis depicted in Figure 13 (b) is founded on the construal of the diminished temperature sensitivities about a thermophysical parameter. The investigation of the reduced sensitivity curves facilitates the identification of the time intervals during which the most accurate estimation of thermal effusivity and volumetric heat capacity can be ascertained. The figure illustrates the relationship between T sensitivity and ρCp and E. The sensitivity of T is limited to the range of 0 to 300 seconds concerning E and becomes sensitive to ρCp after 150 seconds. Therefore, a preliminary estimation of this particular material's activation energy (E) can be determined within 0 to 300 seconds. Conversely, the prediction of ρCp is limited to time intervals of 150 seconds or greater.

Figure 13 (c) demonstrates the convergence of the Tsimul=f(t) and Tsemi-infini=f(t) curves. The findings suggest that the semi-infinite medium assumption holds, thereby enabling the estimation of thermal effusivity. In addition, the pre-estimated value of the volumetric heat capacity can also be evaluated.

3.2. Mechanical Characterization

3.2.1. Compressive Strength

The compressive strength values are 6.3, 8.5, 6.1, and 5.6, respectively, corresponding to 0, 5, 10, and 15% reinforcements in the matrix clay. As illustrated in Figure 14, the only addition of plant aggregates in the matrix clay, which improves the compressive strength, is 5% compared to the compressive strength of the sample without adding plant aggregates. Therefore, the addition of 5% contributes to the improvement of the compressive strength of 35%. The addition of fibers increases compressive strength up to a concentration of 5%, beyond which the strength decreases. Figure 14. The improvement in compressive strength is related to the homogeneous microstructure due to fewer pores. Furthermore, the adequate bonding between the fibers and the clay matrix impedes the propagation of cracks and enhances the compressive strength, as stated in [24]. Several studies have indicated that incorporating plant fibers has led to a notable enhancement in strength [24-28]. In certain instances, the reduction in compressive strength can be attributed to inadequate adhesion between the fibers and the matrix, thereby facilitating the fibers' propensity to slip easily [29, 30]. Furthermore, incorporating plant fibers reduces the substance's dry density, leading to a decline in its strength, as stated in sources [16, 31]. According to previous research [32], there is a negative correlation between porosity and compressive strength, where an increase in porosity results in a decrease in compressive strength. The literature has extensively examined the impact of natural fibers on mechanical

properties. However, it is essential to note that the properties of the specimen being tested, such as size, test method, the composition of the mixture, percentage, and type of fiber, can vary and therefore prevent any generalizations from being made [33].

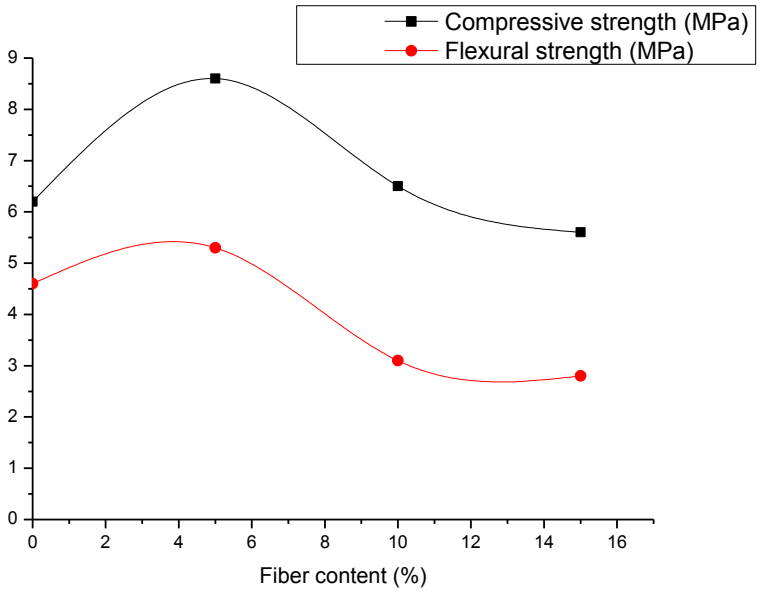

Figure 14. *Compressive and flexural strength as a function of fiber content.*

The thermophysical properties are increasingly improved as the plant aggregate contents increase. The best composition promoting thermal comfort in the building corresponds to a composition reinforced with 15% aggregate additions. Furthermore, the gain in thermal comfort due to improved thermophysical properties is accompanied by the weakening of mechanical properties [24]. However, the lowest compressive strength value (5.6MPa) corresponding to the composition with adding 15% of plant aggregates remains acceptable and slightly higher than 4.5MPa, the recommended compressive strength value for earth bricks to be used in load-bearing walls. The weakening of the mechanical properties despite the improvement in the thermophysical properties of earth briquettes with the addition of plant aggregates has been proven by [24].

3.2.2. Flexural Strength

The findings depicted in Figure 14 indicate that including fibers enhances flexural strength at a 5% fiber concentration. This outcome is consistent with prior research [26, 34-37], demonstrating that incorporating fibers increased tensile and flexural strength across earthen materials. Incorporating kenaf fibers at varying percentages and lengths increased the flexural strength of adobe blocks. This can be attributed to the superior strength of the fibers, as well as their adequate adhesion and distribution within the clay matrix, as reported in [24]. The study found that incorporating banana fibers, particularly those with 60 and 70 mm lengths, enhanced flexural strength, as reported in [25]. According to a study, incorporating kenaf fibers at varying percentages and lengths increased the flexural strength of adobe blocks. This can be attributed to the superior strength of the fibers, as well as their adequate adhesion and distribution within the clay matrix [24].

The incorporation of banana fibers, particularly those with fiber lengths of 60 and 70 mm, has enhanced flexural strength, as reported in [25]. Incorporating 25% sheep's wool resulted in a 30% enhancement in flexural strength, as reported in [26]. This phenomenon is attributed to the fibers' ability to restrict crack propagation through heightened friction at the interface between the fiber and matrix, as noted in [26] and [34]. The elongation of fibers has been noted to be most significant in soils with a high clay content, as documented in [28]. A decrease is observed in the presence of 10% fiber. The incorporation of cotton waste [38] and manioc peel [39] has been found to result in a reduction in flexural strength. The observed phenomenon has been ascribed to several factors, including the heterogeneous nature of the material, insufficient adhesion due to lower cohesive and frictional forces, the brittleness of the fibers, reduction in the volume of the mineral matrix, and decreased compaction resulting from fiber incorporation [15, 40].

3.2.3. Abrasion Coefficient

Figure 15 illustrates the progression of the abrasion coefficient across varying fiber concentrations of 0%, 5%, 10%, and 15%. A meticulous examination of the abovementioned figure reveals that the coefficient exhibits a declining trend

as the fiber content ranges from 0 to 10%, followed by an ascending trend for fiber contents beyond this range.

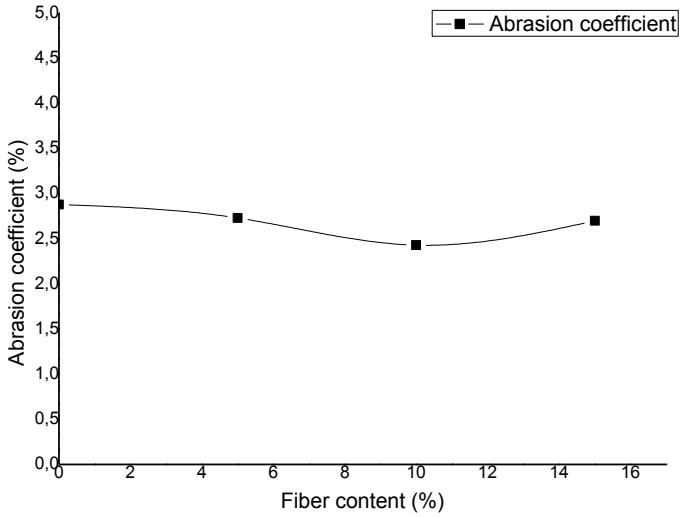

Figure 15. *Abrasion coefficient.*

The findings about the abrasion coefficient are deemed satisfactory, as they suggest that the materials reinforced with fibers exhibit more excellent mechanical durability (in the context of animal contact or rubbing) than the fiberless material. Thus, it can be inferred that incorporating fibers into the soil may yield a favourable or unfavourable outcome regarding the abrasion coefficient [41-43]. Furthermore, the enhanced interfacial adhesion between the fibers and the clay matrix improves material durability, imparting commendable resistance to external erosive forces.

3.2.4. Water Absorption

Figure 16 illustrates the variation of the immersion water absorption coefficient of the material concerning the fiber content evolution. The degree of water absorption of the material exhibits positively correlates with the quantity of fiber present. The augmentation of water absorption resulting from including fibers is primarily attributed to the elevated cellulose concentration within the fibers, which is hydrophilic. The cellulose fibers' absorbent properties facilitate the creation of a conduit within the clay matrix, enabling water to ascend through capillary action [31, 44]. The hydrophilic properties of plant fibers are widely recognized. As reported in previous studies, incorporating natural fibers into stabilized soils has enhanced water absorption owing to their remarkable absorptive capacity [38, 45]. According to Algin and Turgut's research [38], there is a direct relationship between the quantity of cotton waste and the water absorption level.

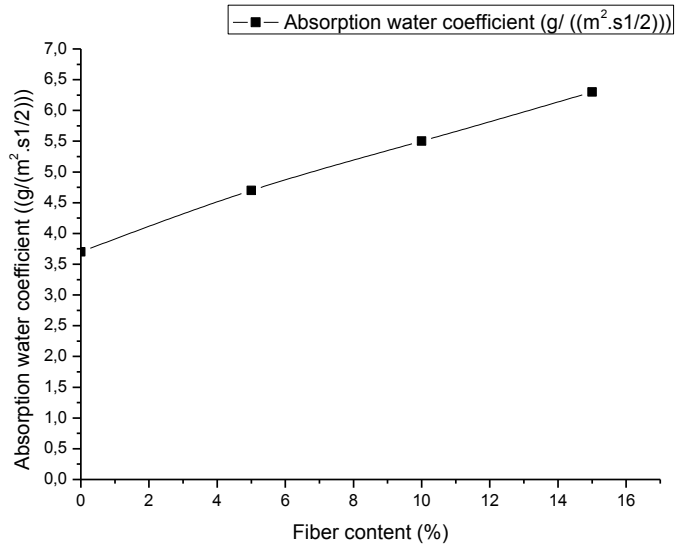

Figure 16. *Absorption water coefficient in the function of fibre content.*

A 40% increase in cotton content (by volume) resulted in a doubling of the water absorption capacity of the material, from 12.5% to 27.2%. The absorption phenomenon is crucial in determining the fibers' and matrix adhesion characteristics. Water absorption causes the swelling of fibers, resulting in soil repulsion, and conversely, the reduction in fiber volume during drying, leading to voids around them, has been documented [46].

4. Conclusion

The primary aim of this research was to investigate the mechanical and thermophysical properties of utilizing plant fibers to enhance energy efficiency in buildings. The introduction of plant fibers at varying percentages (0%, 5%, 10%, and 15%) yielded positive results in several aspects:

Incorporating plant aggregates in different percentages resulted in a 45% reduction in thermal conductivity compared to samples without reinforcement. An inverse relationship between fiber size and thermal conductivity was observed, which is advantageous in climates with high temperatures, reaching up to 50 ℃.

The compressive strength values were as follows: 6.3 MPa for 0% reinforcement, 8.5 MPa for 5% reinforcement, 6.1 MPa for 10% reinforcement, and 5.6 MPa for 15% reinforcement in the clay matrix. Adding 5% fibers led to a 35% improvement in compressive strength. However, beyond the 5% concentration, the strength began to decrease. Mud bricks with a compressive strength between 2 and 4 MPa are suitable for non-load-bearing walls, while those with a compressive strength above 4 MPa are recommended for load-bearing walls. The materials do not have any disadvantages when used as load-bearing walls.

Our research has various applications, including:

Due to the thermal and moisture-regulating properties of our materials, we are creating structures capable of withstanding extreme climatic events.

To support sustainable living, construct resilient housing in rural areas vulnerable to natural disasters.

We use our materials to renovate and restore historic buildings while preserving their architectural integrity.

This work is subject to limitations due to laboratory conditions that imposed dimensions and formed samples that differ from those used by the craftsmen. Studying the microstructure and chemical and mineralogical composition of the materials used is essential to understanding the relationship between the soil matrix and plant aggregates and analyzing their acoustic properties.

Abbreviations

WEO	World Energy Outlook
ASTM	American Society for Testing and Materials

Acknowledgments

The authors thank the Laboratory of Water, Energy and Environment (L3E) at the National Advanced School of Engineering in Yaoundé, for the thermal findings derived from this laboratory. In addition, the authors thank the Local Materials Promotion Agency (MIPROMALO), for providing access to their laboratory, where mechanical characterizations were conducted.

Conflicts of Interest

The authors declare no conflicts of interest.

References

[1] C. Llatas, "A model for quantifying construction waste in projects according to the European waste list," *Waste Manag.*, vol. 31, no. 6, pp. 1261–1276, 2011, https://doi.org/10.1016/j.wasman.2011.01.023

[2] C. Thormark, "The effect of material choice on the total energy need and recycling potential of a building," *Build. Environ.*, vol. 41, no. 8, pp. 1019–1026, 2006, https://doi.org/10.1016/j.buildenv.2005.04.026

[3] H. Van Damme and H. Houben, "Earth concrete. Stabilization revisited," *Cem. Concr. Res.*, vol. 114, pp. 90–102, 2018, https://doi.org/10.1016/j.cemconres.2017.02.035

[4] N. Kouta, J. Saliba, and N. Saiyouri, "Effect of flax fibers on early age shrinkage and cracking of earth concrete," *Constr. Build. Mater.*, vol. 254, p. 119315, 2020, https://doi.org/10.1016/j.conbuildmat.2020.119315

[5] E. O. Momoh and A. I. Osofero, "Behaviour of oil palm broom fibers (OPBF) reinforced concrete," *Constr. Build. Mater.*, vol. 221, pp. 745–761, 2019, https://doi.org/10.1016/j.conbuildmat.2019.06.118

[6] N. Benmansour, B. Agoudjil, A. Gherabli, A. Kareche, and A. Boudenne, "Thermal and mechanical performance of natural mortar reinforced with date palm fibers for use as insulating materials in building," *Energy Build.*, vol. 81, pp. 98–104, 2014, https://doi.org/10.1016/j.enbuild.2014.05.032

[7] J. C. Damfeu, P. Meukam, Y. Jannot, and E. Wati, "Modelling and experimental determination of thermal properties of local wet building materials," *Energy Build.*, vol. 135, pp. 109–118, 2017, https://doi.org/10.1016/j.enbuild.2016.11.022

[8] F. R. de Hoog, J. H. Knight, and A. N. Stokes, "An Improved Method for Numerical Inversion of Laplace Transforms," *SIAM J. Sci. Stat. Comput.*, vol. 3, no. 3, pp. 357–366, 1982, https://doi.org/10.1137/0903022

[9] E. Hamard, B. Cazacliu, A. Razakamanantsoa, and J. C. Morel, "Cob, a vernacular earth construction process in the context of modern sustainable building," *Build. Environ.*, vol. 106, pp. 103–119, 2016, https://doi.org/10.1016/j.buildenv.2016.06.009

[10] S. Liuzzi *et al.*, "Hygrothermal properties of clayey plasters with olive fibers," *Constr. Build. Mater.*, vol. 158, pp. 24–32, 2018, https://doi.org/10.1016/j.conbuildmat.2017.10.013

[11] J. Lima, P. Faria, and A. S. Silva, "Earthen plasters based on illicit soils from barrel region of Algarve: Contributions for building performance and sustainability," *Key Eng. Mater.*, vol. 678, pp. 64–77, 2016, https://doi.org/10.4028/www.scientific.net/KEM.678.64

[12] M. I. Gomes, P. Faria, and T. D. Gonçalves, "Earth-based mortars for repair and protection of rammed earth walls. Stabilization with mineral binders and fibers," *J. Clean. Prod.*, vol. 172, pp. 2401–2414, 2018, https://doi.org/10.1016/j.jclepro.2017.11.170

[13] M. Palumbo, F. McGregor, A. Heath, and P. Walker, "The influence of two crop by-products on the hygrothermal properties of earth plasters," *Build. Environ.*, vol. 105, pp. 245–252, 2016, https://doi.org/10.1016/j.buildenv.2016.06.004

[14] A. Simons *et al.*, "Development of bio-based earth products for healthy and sustainable buildings: Characterization of microbiological, mechanical and hygrothermal properties," *Mater. Tech.*, vol. 103, no. 2, 2015, https://doi.org/10.1051/match/2015011

[15] A. Ledhem, R. M. Dheilly, M. L. Benmalek, and M. Quéneudec, "Properties of wood-based composites formulated with aggregate industry waste," *Constr. Build. Mater.*, vol. 14, no. 6–7, pp. 341–350, 2000, https://doi.org/10.1016/S0950-0618(00)00037-4

[16] K. Al Rim, A. Ledhem, O. Douzane, R. M. Dheilly, and M. Queneudec, "Influence of the proportion of wood on the thermal and mechanical performances of clay-cement-wood composites," *Cem. Concr. Compos.*, vol. 21, no. 4, pp. 269–276, 1999, https://doi.org/10.1016/S0958-9465(99)00008-6

[17] A. Laborel-Préneron, C. Magniont, and J. E. Aubert, "Hygrothermal properties of unfired earth bricks: Effect of barley straw, hemp shiv, and corn cob addition," *Energy Build.*, vol. 178, pp. 265–278, 2018, https://doi.org/10.1016/j.enbuild.2018.08.021

[18] A. Limam, A. Zerizer, D. Quenard, H. Sallee, and A. Chenak, "Experimental thermal characterization of bio-based materials (Aleppo Pine wood, cork, and their composites) for building insulation," *Energy Build.*, vol. 116, pp. 89–95, 2016, https://doi.org/10.1016/j.enbuild.2016.01.007

[19] M. Boumhaout, L. Boukhattem, H. Hamdi, B. Benhamou, and F. Ait Nouh, "Thermomechanical characterization of a bio-composite building material: Mortar reinforced with date palm fibers mesh," *Constr. Build. Mater.*, vol. 135, pp. 241–250, 2017, https://doi.org/10.1016/j.conbuildmat.2016.12.217

[20] A. Djoudi, M. M. Khenfer, A. Bali, and T. Bouziani, "Effect of the addition of date palm fibers on thermal properties of plaster concrete: Experimental study and modeling," *J. Adhes. Sci. Technol.*, vol. 28, no. 20, pp. 2100–2111, 2014, https://doi.org/10.1080/01694243.2014.948363

[21] M. Bederina, L. Marmoret, K. Mezreb, M. M. Khenfer, A. Bali, and M. Quéneudec, "Effect of the addition of wood shavings on thermal conductivity of sand concretes Experimental study and modeling," *Constr. Build. Mater.*, vol. 21, no. 3, pp. 662–668, 2007, https://doi.org/10.1016/j.conbuildmat.2005.12.008

[22] H. Shoukry, M. F. Kolkata, S. A. Abo-EL-Enein, M. S. Morsy, and S. S. Shebl, "Thermo-physical properties of nanostructured lightweight fiber reinforced cementitious composites," *Constr. Build. Mater.*, vol. 102, pp. 167–174, 2016, https://doi.org/10.1016/j.conbuildmat.2015.10.188

[23] J. Khedari, B. Suttisonk, N. Pratinthong, and J. Hirunlabh, "New lightweight composite construction materials with low thermal conductivity," *Cem. Concr. Compos.*, vol. 23, no. 1, pp. 65–70, 2001, https://doi.org/10.1016/S0958-9465(00)00072-X

[24] Y. Millogo, J. C. Morel, J. E. Aubert, and K. Ghavami, "Experimental analysis of Pressed Adobe Blocks reinforced with Hibiscus cannabinus fibers," *Constr. Build. Mater.*, vol. 52, pp. 71–78, 2014, https://doi.org/10.1016/j.conbuildmat.2013.10.094

[25] M. Mostafa and N. Uddin, "Experimental analysis of Compressed Earth Block (CEB) with banana fibers resisting flexural and compression forces," *Case Stud. Constr. Mater.*, vol. 5, pp. 53–63, 2016, https://doi.org/10.1016/j.cscm.2016.07.001

[26] C. Galán-Marín, C. Rivera-Gómez, and J. Petric, "Clay-based composite stabilized with natural polymer and fiber," *Constr. Build. Mater.*, vol. 24, no. 8, pp. 1462–1468, 2010, https://doi.org/10.1016/j.conbuildmat.2010.01.008

[27] H. Binici, O. Aksogan, M. N. Bodur, E. Akca, and S. Kapur, "Thermal isolation and mechanical properties of fiber reinforced mud bricks as wall materials," *Constr. Build. Mater.*, vol. 21, no. 4, pp. 901–906, 2007, https://doi.org/10.1016/j.conbuildmat.2005.11.004

[28] M. Bouhicha, F. Aouissi, and S. Kenai, "Performance of composite soil reinforced with barley straw," *Cem. Concr. Compos.*, vol. 27, no. 5, pp. 617–621, 2005, https://doi.org/10.1016/j.cemconcomp.2004.09.013

[29] E. Quagliarini and S. Lenci, "The influence of natural stabilizers and natural fibers on the mechanical properties of ancient Roman adobe bricks," *J. Cult. Herit.*, vol. 11, no. 3, pp. 309–314, 2010, https://doi.org/10.1016/j.culher.2009.11.012

[30] J. Khedari, P. Watsanasathaporn, and J. Hirunlabh, "Development of fiber-based soil-cement block with low thermal conductivity," *Cem. Concr. Compos.*, vol. 27, no. 1, pp. 111–116, 2005, https://doi.org/10.1016/j.cemconcomp.2004.02.042

[31] K. Ghavami, R. D. Toledo Filho, and N. P. Barbosa, "Behaviour of composite soil reinforced with natural fibers," *Cem. Concr. Compos.*, vol. 21, no. 1, pp. 39–48, 1999, https://doi.org/10.1016/S0958-9465(98)00033-X

[32] A. Bouguerra, A. Ledhem, F. Barquin, R. M. Dheilly, and M. Queneudec, "Effect of Microstructure on the Mechanical and Thermal," *Cem. Concr. Res.*, vol. 28, no. 8, pp. 1179–1190, 1998.

[33] A. Laborel-Préneron, J. E. Aubert, C. Magniont, C. Tribout, and A. Bertron, "Plant aggregates and fibers in earth construction materials: A review," *Constr. Build. Mater.*, vol. 111, pp. 719–734, 2016, https://doi.org/10.1016/j.conbuildmat.2016.02.119

[34] F. Aymerich, L. Fenu, and P. Meloni, "Effect of reinforcing wool fibers on fracture and energy absorption properties of an earthen material," *Constr. Build. Mater.*, vol. 27, no. 1, pp. 66–72, 2012, https://doi.org/10.1016/j.conbuildmat.2011.08.008

[35] A. E. M. K. Mohamed, "Improvement of swelling clay properties using hay fibers," *Constr. Build. Mater.*, vol. 38, pp. 242–247, 2013, https://doi.org/10.1016/j.conbuildmat.2012.08.031

[36] Y. Millogo, J. E. Aubert, E. Hamard, and J. C. Morel, "How properties of kenaf fibers from Burkina Faso contribute to the reinforcement of earth blocks," *Materials (Basel).*, vol. 8, no. 5, pp. 2332–2345, 2015, https://doi.org/10.3390/ma8052332

[37] D. LEVACHER, F. WANG, and Y. LIANG, "Co-valorisation de matériaux fins et sédiments," pp. 869–876, 2010, https://doi.org/10.5150/jngcgc.2010.094-l

[38] H. M. Algin and P. Turgut, "Cotton and limestone powder wastes as brick material," *Constr. Build. Mater.*, vol. 22, no. 6, pp. 1074–1080, 2008, https://doi.org/10.1016/j.conbuildmat.2007.03.006

[39] M. C. N. Villamizar, V. S. Araque, C. A. R. Reyes, and R. S. Silva, "Effect of the addition of coal-ash and cassava peels on the engineering properties of compressed earth blocks," *Constr. Build. Mater.*, vol. 36, pp. 276–286, 2012, https://doi.org/10.1016/j.conbuildmat.2012.04.056

[40] Ş. Yetgin, Ö. ÇAVDAR, and A. Çavdar, "The effects of the fiber contents on the mechanic properties of the adobes," *Constr. Build. Mater.*, vol. 22, no. 3, pp. 222–227, 2008, https://doi.org/10.1016/j.conbuildmat.2006.08.022

[41] P. M. Toure, V. Sambou, M. Faye, and A. Thiam, "Mechanical and thermal characterization of stabilized earth bricks," *Energy Procedia*, vol. 139, pp. 676–681, 2017, https://doi.org/10.1016/j.egypro.2017.11.271

[42] M. Ali, "Microstructure, Thermal Analysis and Acoustic Characteristics of Calotropis procera (Apple of Sodom) Fibers," *J. Nat. Fibers*, vol. 13, no. 3, pp. 343–352, 2016, https://doi.org/10.1080/15440478.2015.1029198

[43] I. Demir, "An investigation on the production of construction brick with processed waste tea," *Build. Environ.*, vol. 41, no. 9, pp. 1274–1278, 2006, https://doi.org/10.1016/j.buildenv.2005.05.004

[44] H. Danso, B. Martinson, M. Ali, and C. Mant, "Performance characteristics of enhanced soil blocks: A quantitative review," *Build. Res. Inf.*, vol. 43, no. 2, pp. 253–262, 2015, https://doi.org/10.1080/09613218.2014.933293

[45] B. Taallah, A. Guettala, S. Guettala, and A. Kriker, "Mechanical properties and hygroscopicity behavior of compressed earth block filled by date palm fibers," *Constr. Build. Mater.*, vol. 59, pp. 161–168, 2014, https://doi.org/10.1016/j.conbuildmat.2014.02.058

[46] M. Segetin, K. Jayaraman, and X. Xu, "Harakeke reinforcement of soil-cement building materials: Manufacturability and properties," *Build. Environ.*, vol. 42, no. 8, pp. 3066–3079, 2007, https://doi.org/10.1016/j.buildenv.2006.07.033